Effect of $AgNO_3$ incorporation on the mixture of chlorophylls, anthocyanins, and betalains dyes on dye-sensitized solar cell performance

FAHRU NUROSYID*, UNTUNG RIYADI, HENDRY WIDIYANDARI, YOFENTINA IRIANI, AGUS SUPRIYANTO
Department of Physics, Faculty of Mathematics and Natural Sciences Faculty, Sebelas Maret University, Jl. Ir. Sutami 36A, Kentingan, Surakarta 57126, Indonesia

In this study, anthocyanins (A), betalain (B), and chlorophyll (C) were extracted from natural sources. Each dye was combined (volume ratios of 1:1) and labeled AB, AC, BC, and ABC. The ABC dyes were incorporated with $AgNO_3$ in various concentrations to improve the photovoltaic performance. The optical properties of the prepared dyes, the morphology of the TiO2 layers containing the prepared dyes, and the photovoltaic performance of developed DSSCs were evaluated. The results revealed that fabricated DSSCs composing ABC incorporated with 3 mM $AgNO_3$ yielded the best conversion efficiency as doping can induce faster electron transport. It demonstrated that $AgNO_3$-incorporated ABC, with the lowest Ag concentration, was the best dye modification to produce with an efficiency of 1.635 %. This is because Ag has good conductivity properties, so the higher concentration added may increase the conductivity of the TiO_2.

(Received June 29, 2024; accepted December 2, 2024)

Keywords: DSSC, Natural dye combination, Ag concentration, Optical properties, Electrical performance

1. Introduction

In the last few decades, energy needs have increased so that sustainable and environmentally friendly energy is needed. One of the renewable energies is solar light, which Indonesia receives relatively high light intensity every year, around 4.8 kWh/m^2. Thus, it has significant potential for photovoltaic applications. Dye-Sensitized Solar Cell (DSSC) is a third-generation solar cell consisting of a nanostructured electrochemical photo device that directly absorbs sunlight and converts it into electrical energy, first developed by O'Regan and Grätzel in 1991.

Compared to conventional solar cells, the DSSC possesses the advantages of easy manufacturing processes, inexpensive materials, lightweight and flexible, simple preparation technique, and environmentally friendly. Therefore, it has the potential as an energy conversion technology, where its conversion efficiency can be improved to a higher level [1]. Nevertheless, DSSC has the drawbacks of relatively low efficiency, low scalability, and high costs of ruthenium dye, electrodes, and conducting glass. The DSSC structure generally comprises a photoanode, dye, electrolyte, counter electrode, and glass substrate. TiO_2 is often used as a photoanode coated on FTO glass substrates. Dye is a crucial component in DSSC because it plays a direct role in the absorption of sunlight, photoelectron production, and electron transfer to increase the conversion efficiency of solar cells. The dye is helpful in absorbing light, and electrons from the dye are injected into TiO_2. Besides, it plays a vital role in exciton generation and injection of electrons into electron acceptors, which determines the short circuit current density (J_{sc}) [2-3].

An ideal DSSC dye must have visible light absorption, resulting in a high molar absorption coefficient. Besides, the dye can bind to the semiconductor through retaining groups, which causes electron injection and faster transfer of electrons to the semiconductor [4]. Two types of dyes are commonly used in DSSC fabrication: synthetic and natural. Synthetic dyes generally use ruthenium complexes because of their excellent ability to absorb visible light and their high efficiency in metal-ligand charge transfer transitions. The synthetic dye N719 Ruthenium has a high efficiency of around 11.7%, and the black dye N749 reaches 11.15% [5]. However, the availability of synthetic dye is limited, the price is expensive, the synthesis is quite complicated, and it is toxic [6]. Therefore, natural dyes are employed because they are abundant in nature, easy to obtain and synthesize, and environmentally friendly compared to synthetic dyes. However, natural dyes still have relatively narrow absorption at wavelengths, producing low DSSC efficiency [7].

The light absorption properties of natural dyes can be improved by modifying the dyes, giving varying colors, thereby changing the wavelength absorption area. Natural dyes mixture can absorb a wider light spectrum than single dyes [4]. Pratiwi's study of dye modification by mixing chlorophyll and anthocyanin extracts revealed excellent light absorption in the long wavelength range and an efficiency of 0.154% [8]. Besides, Sinha's research using three mixed dyes from extracts of turmeric stems, purple cabbage, and spinach leaves had an efficiency of 0.602% due to the absorption of a broad solar spectrum and an excellent electrochemical response, increasing efficiency [5].

To further enhance the DSSC efficiency, the dyes can be inserted by metal elements through doping. Research conducted on Ni metal doping into chlorophyll dye revealed increased electrical conductivity and absorbance, resulting in an efficiency of up to 135% compared to pure chlorophyll [9]. Transition metal doping in dye can increase the dye's energetic and kinetic properties, thereby improving the performance of DSSC.

Current studies focus on Ag doping on dyes for DSSC. The insertion of Ag ions increases the electrical conductivity and reduces the energy during the excitation process by absorbing more photons. In addition, it reduces charge recombination due to induced Schottky barriers at the interface of the charge carriers generated by the photons, thereby increasing the electron density in the conduction band [10]. The use of Ag can effectively improve the optical absorption of DSSC, and it has good thermal and electrical conductivity. This research focuses on widening the dye's absorption area to increase the natural injection of photoelectrons and reduce recombination in DSSC. This research has the novelty of combining three dye mixtures of anthocyanin, betalain, and chlorophyll. Further, the three mixed dyes were incorporated with $AgNO_3$ to improve the conversion efficiency of DSSC.

This study used the natural dyes of anthocyanin, betalain, and chlorophyll. Anthocyanin dye was extracted from dragon fruit peel due to its high anthocyanin content of 21.9757% and low production costs [14]. Betalain dye was obtained from Bougainvillea glabra extraction, which has a purple color, contains 6.78 mg/g of betalain, and has the advantages of being pH-independent and more stable. Betalain pigments can increase efficiency by up to 1.92% and photocurrent of 2.11% compared to chlorophyll [6]. Chlorophyll dye was extracted from cassava leaves because it has the best chlorophyll content of 27.4467 mg/g [15, 16]. Chlorophyll has a LUMO energy level value higher than the TiO_2 conduction band energy level, which can facilitate electron transfer to the conduction band.

2. Method

For manufacturing DSSC devices, this study employed Fluoride Thin Oxide (FTO, DyeSol) for the substrate, Titanium Dioxide Paste 18NRT (gretcell) for the working electrode, Platinum paste (Dyesol) as the counter electrode, electrolyte (EL- UHSE, DyeSol), silver nitrate ($AgNO_3$) (Sigma Aldrich) as the doping material for the working electrode, and dye extracts from three natural sources. The tree dyes were chlorophyll, betalain, and anthocyanin.

Anthocyanin dye (labeled A) was obtained from dragon fruit (Hylocereus polyrhizus) peel extract using methanol and acetic acid solvents. Betalain dye solution extract (B) was from Bougainvillea glabra with acetone and methanol solvents. The chlorophyll dye solution (C) was extracted from cassava leaves (Manihot esculenta) with distilled water and ethanol solvents. Each dye was mixed with a volume ratio of 1:1, including anthocyanin-betalain (AB), betalain-chlorophyll (BC), anthocyanin-chlorophyll (AC), and anthocyanin-betalain-chlorophyll (ABC). ABC dye was incorporated with Ag ions with various $AgNO_3$ concentrations of 3 mM (Ag1), 30 mM (Ag2), and 300 mM (Ag3).

For DSSC assembly, the layer of TiO_2 was immersed in dye solutions (A, B, C, AB, BC, AC, ABC, ABC-Ag1, ABC-Ag2, ABC-Ag3) for about 24 hours and kept out of direct sunlight. The platinum paste counter electrode was deposited onto the conductive side of the FTO substrate layer using the spin coating method at 2000 rpm for 60 seconds. Thin films ready for counter electrodes and photoanodes were arranged to form sandwiches. An electrolyte solution (EL-UHSE) was injected into the gaps of the cells in an active area. Before testing, the DSSC sandwich structure was coated with a keyboard protector on the left and right sides of the area between the two electrodes. The purpose of the coating was to prevent short contact. The opposing electrode was dripped with electrolyte first, and the working electrode was stacked on top of it.

The power conversion efficiency of prepared DSSCs was obtained using Eq. 1 (Hou et al., 2013).

$$\eta = \frac{V_{oc} J_{sc} FF}{P_{in}} \text{x } 100\% \quad (1)$$

P_{in} is incident light intensity (1000 watt/m^2), while the DSSC active area was 0.000025 m^2, so that J_{sc}=I (10^{-3})A/ 0.000025 m^2, where the unit of V_{oc} is Volt and J_{sc} is Ampere/m^2.

The absorbance of the dye solutions was measured using a Hitachi UH-5300 UV-visible Spectrophotometer. Fourier Transform Infra-Red (FTIR) spectroscopy (FTIR Prestige-21 Shimadzu type 8201PC) was employed for atomic bond evaluation at 400 – 4000 cm^{-1} wavenumber. The conductivity of the Ag-incorporated ABC dye solutions was estimated using the two-probe method. The DSSC performance was evaluated via the IV meter Keithley 2602 system source with light intensity at 1000 W/m^2.

3. Results and discussion

3.1. Optical properties of pure and Ag-incorporated dyes solutions

The UV-visible absorption spectra of the extracted dyes are shown in Fig. 1. The characterization peak at 522 nm indicates the presence of red-purple anthocyanin pigments in the Hylocereus polyrhizus extract. The anthocyanin absorption area is located on the strong absorption of 455-580 nm, which is in visible light ranges [14,8]. The absorption peak denotes that many electrons are excited due to the light absorption by the dye molecules [17].

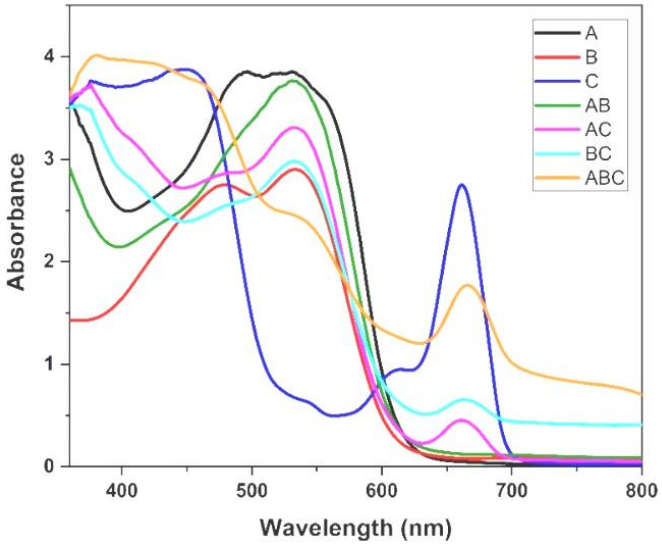

Fig. 1. Absorption spectra of single and mixed dyes (color online)

The main peak of Betalain dye extracted from bougainvillea glabra flower is found at a wavelength of 481.5 nm that can be associated with indicaxathin. Meanwhile, the second peak at a wavelength of 526 nm identifies the presence of betanin [18, 19]. The wide absorption area of betalain in the wavelength range of 480-560 nm follows research by Isah et al. [18]. It occurs when there is a transition from $\pi-\pi*$ due to the presence of a mixture of betaxanthins (yellow-orange) and betanin (red-purple) [18]. For chlorophyll dye (C), the peak absorbance values at 433.5 nm and 657 nm wavelengths represent dye extract from Manihot esculenta leaves (C). Meanwhile, peaks at wavelengths of 410 nm, 430 nm, and 675 nm indicate the presence of chlorophyll [20, 21].

The anthocyanin-betalain (AB) mixture has an absorption area of around 470-620 nm, which the absorption increase compared to the single dye of anthocyanin or betalain. Anthocyanin-betalain (AB) used distilled water and ethanol solvents in the extraction, presented at 400 nm and 570 wavelengths, respectively. The absorption spectrum of the mixture is almost the same as that of bougainvillea glabra flower extract, with a wider absorption range and higher peak intensity at 532.5 nm [22].

Likewise, the spectrum of the anthocyanin-chlorophyll (AC) mixture causes a widening of the absorption region of 400-700 nm. The AC mixture has 3 absorbance peaks at wavelengths of 410 nm, 537 nm, and 666.5 nm. This is due to the addition of anthocyanins, which have a wide absorption spectrum ranging from 450 to 580 nm depending on the plant or solvent used [23]. Anthocyanin-chlorophyll dye can expand the absorbance area, but the absorbance value is reduced. This is because chlorophyll works optimally at pH 7-8, while anthocyanins have a relatively low pH of 1-5, so the work tends to decrease at extreme pH [24]. The combination of betalain-chlorophyll (BC) dye is obtained at absorbance peaks at 411 nm and 666.5 nm, corresponding to chlorophyll, and at 523 nm, indicating betanin pigment.

The mixture of dragon fruit peel dye, bougainvillea glabra flowers, and Manihot esculenta leaves (ABC) has high absorption peaks at wavelengths of 474.5 nm (betalain dye contribution), 536.5 nm (anthocyanin dye), 608.5 nm (betalain dye), 666 nm (chlorophyll dye). The three mixed dyes exhibit a broad spectrum of light absorption characteristics. The light absorption area ranges from 410 nm to 700 nm. Besides, the ABC spectrum shows all the peaks from each single dye with strong absorption, especially in the middle area. The broader and stronger light absorption of mixed dyes tends to provide higher efficiency than single dyes [25]. The difference in the solvents used to extract dyes affects the dye mixture. Ethanol and acetone solvents for chlorophyll extract have a lower polarity level than acetic acid, methanol, and distilled water solvents in extracting anthocyanins, resulting in peak shifts and changes in absorbance levels. The absorption area experiences a shift towards a larger wavelength due to the addition of solvent and the number of auxochrome groups [9]. Finally, it shows that the mixture of three dyes can increase the absorbance of each single dye, indicating improved light absorption intensity (hyperchromic effect) [26].

The bandgap of the pure TiO_2 layer and layers of TiO_2+ABC and TiO_2+ABC/Ag is presented in Fig. 2. The bandgap value of the pure TiO_2 layer is 3.3 eV which is close to the bandgap value of TiO_2 anatase phase [27,28]. The bandgap value of TiO_2 immersed in ABC dye is smaller than that of pure TiO_2 (3.2 eV). This condition indicates that the dye has an amorphous structure, which can reduce the bandgap value. It then results in maximum photon absorption and accelerating electron transfer from the valence band to the conduction band [29,13]. Further, the immersion of TiO_2 into $AgNO_3$-incorporated ABC dyes decreases the energy band gap value to 3.0 eV. This

is because the conductivity of the dye increases, resulting in the reduced bandgap of the layer [13].

Besides, the addition of Ag metal in the dye acts as a donor atom, so the Fermi energy will shift towards the conduction band, resulting in a declined energy bandgap [30].

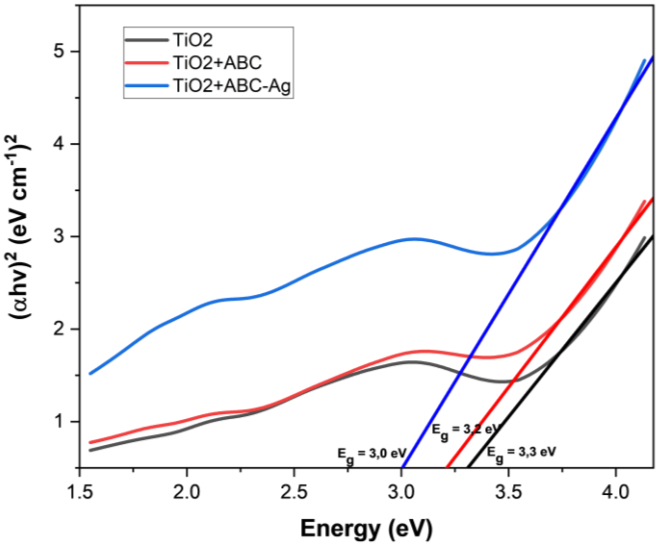

Fig. 2. Bandgap of pure TiO_2 layers and layers of TiO_2+ABC and TiO_2+ABC/Ag (color online)

3.2. Morphological structure

The morphology images of the TiO_2 layer and the TiO_2+Ag-incorporated ABC dye are depicted in Fig. 3. It presents that pure TiO_2 has a porous morphology (Fig. 3a), where the more porous morphology can enhance the possibility for dye molecules to be adsorbed onto its surface [30]. Besides, the smaller particle size will cause the number of pores to increase, easing the spread of the electrolyte solution. It finally induces a greater efficiency because more electron-hole pairs are produced [31].

The uniformity of the TiO_2 coating on the FTO substrate also greatly influences its electrical characteristics, relating to the enhanced efficiency of the light obtained during the process [32]. Fig. 3b depicts the morphology image of TiO_2 immersed in ABC dye. The figure shows that the layer has a tiny nanorod particle shape. A noticeable difference is demonstrated in the TiO_2 layer immersed in $AgNO_3$-incorporated ABC at 300 nM Ag concentration. It denotes that an excessive $AgNO_3$ concentration can damage the crystal structure because an excessive concentration of $AgNO_3$ may tend to cover the top surface of the TiO_2 layer, inducing atomic defects.

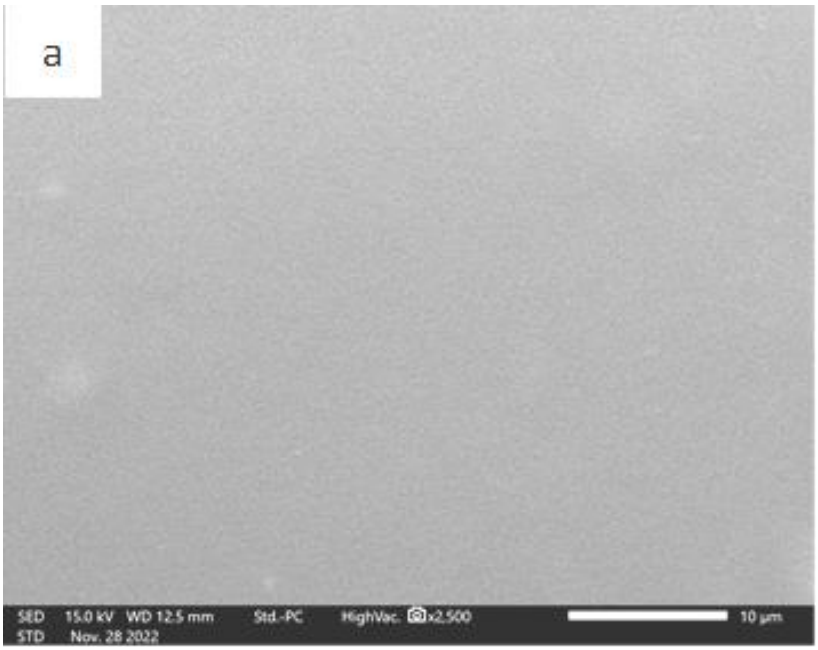

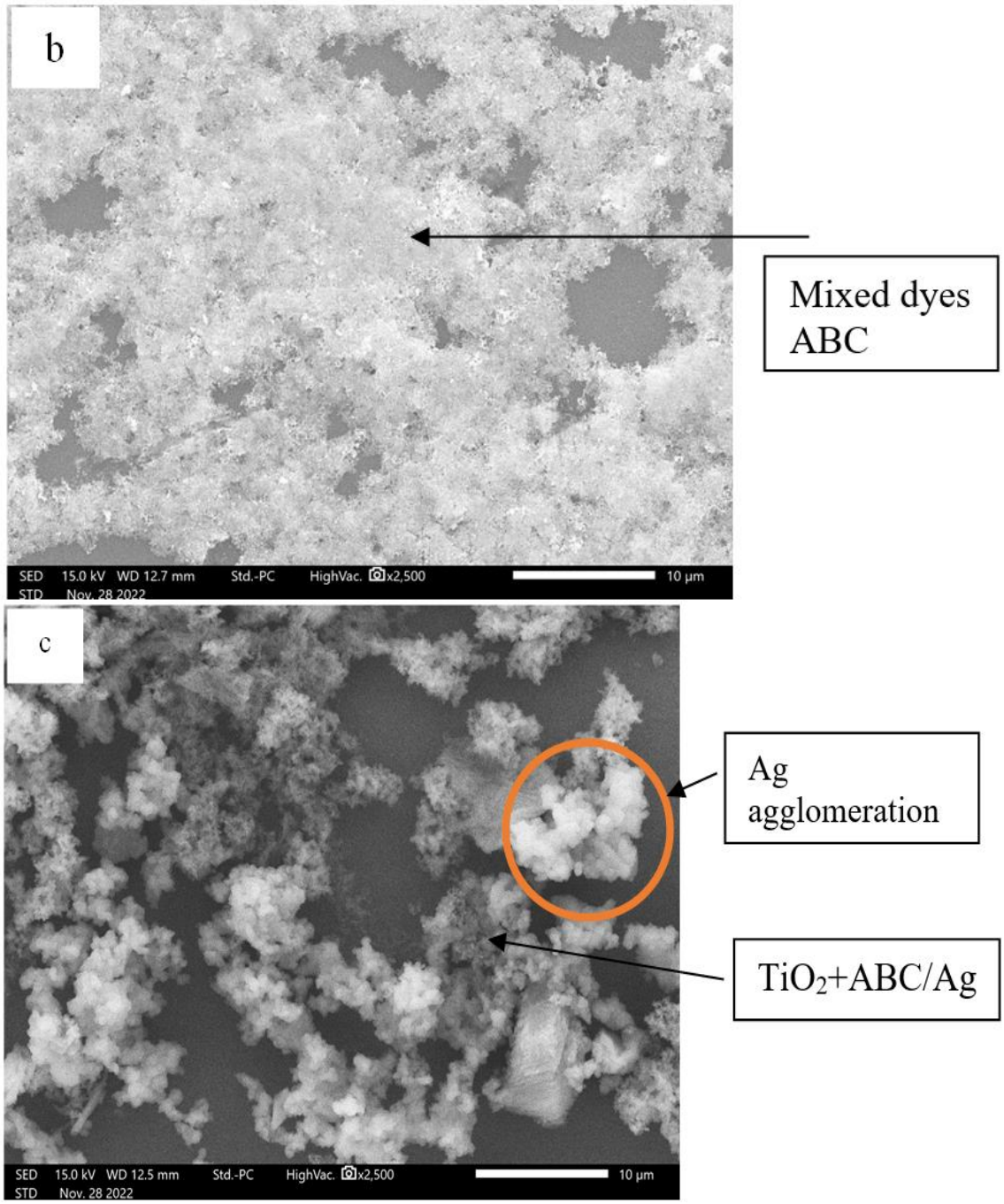

Fig. 3. Morphology images of (a) pure TiO_2, (b) TiO_2+ABC, and (c) TiO_2+ABC/ $AgNO_3$

3.3. FTIR analysis

The functional groups of single dyes, mixed dyes, and Ag-incorporated ABC are shown in Fig. 4. The O-H stretching vibration at about 3550–3200 cm^{-1} shows a strong and broad peak intensity, denoting the presence of the hydroxy group. The C-H stretching vibration at 2990–2850 cm^{-1} refers to the presence of alkanes. The C≡C stretching vibration at 2250–2100 cm^{-1} is associated with the existence of aromatic compounds. The C=C bending at 1660–1600 cm^{-1} denotes the presence of alkenyl. The C-O stretching vibration at 2250–2100 cm^{-1} represents the appearance of aromatic compounds. The C-N stretching vibration at 1350–1000 cm^{-1} indicates the existence of amine. The C-H bending at 840–790 cm^{-1} reveals a disubstituted bending spectrum pattern from the presence of alkenes. In $AgNO_3$-incorporated (ABC), the peak at 803 cm^{-1} emerges, denoting the wavenumber of Ag metal [30].

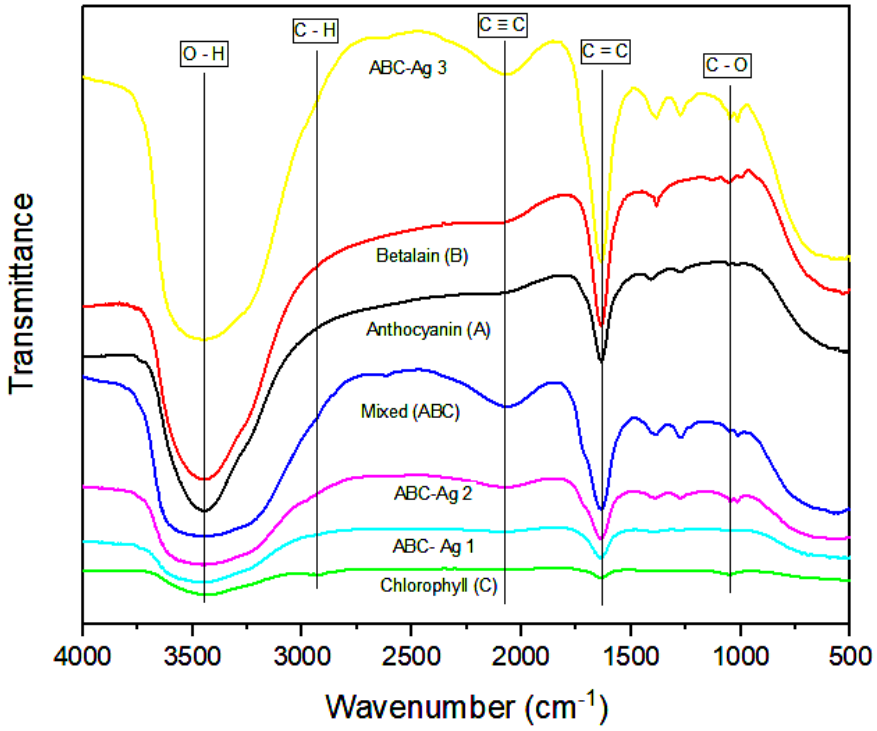

Fig. 4. FTIR spectra of single dye, mixed dyes, and Ag-incorporated mixed dyes (color online)

Overall, the O-H stretching vibration in the spectra indicates a hydroxyl group, while the C-O stretching vibration denotes the ester compound containing a carbonyl group. Hydroxyl and carbonyl functional groups also play a role in the TiO_2 semiconductor binding process [7]. Therefore, the presence of hydroxyl and carbonyl functional groups can optimize the electron injection from HOMO to LUMO.

3.4. Conductivity of dye solutions

The conductivity curves of the dye solutions in dark and light conditions are presented in Fig. 5. Table 1 demonstrates that the conductivity of three mixed dyes (ABC) in the dark conditions is 0.4678 $\Omega^{-1}m^{-1}$, which increases to 0.9149 $\Omega^{-1}m^{-1}$ in the light condition. Further, it exhibits that the conductivity values of the dye solution rise linearly with the addition of higher Ag concentration. The higher conductivity of the dyes induces the easier electron donor ability. The electrical conductivity of a solution depends on the concentration, type, and number of ions present in the solution. The electric current in the solution is conducted by the ions contained in it [14]. The higher Ag ion concentration leads to more ions in the solution, enhancing its electrical conductivity. If the conductivity value of Ag-incorporated mixed dyes increases compared to those without Ag doping, this identifies the formation of ionic compounds. Ionic compounds play an essential role in conducting electricity because they are easily broken down into ions due to the continuous electron transfer process, so they are suitable for application to DSSC [31]. This indicates that the Ag-incorporated mixed dyes have good sensitizing properties, so the mixed dye can better be applied as a DSSC photosensitizer.

3.5. Current-voltage measurements (performance of DSSC)

Table 2 shows the photovoltaic parameters of the DSSC using anthocyanin, betalain, and chlorophyll dyes of 0.193%, 0.225%, and 0.228%, respectively. DSSC with anthocyanin dye is more efficient than betalain and chlorophyll dyes. Fig. 6 depicts that dragon fruit peel (A), containing anthocyanin pigment, has a relatively low J_{sc} value of 9.04 Am^{-2}. Nevertheless, it can provide a higher open circuit voltage of 0.469 V with a fill factor of 0.456. Dye betalain shows a slightly higher J_{sc} value of 18.86 Am^{-2}, open circuit voltage of 0.394 V, fill factor of 0.375, and efficiency of 0.228. Chlorophyll dye exhibits a lower J_{sc} value than betalain of 13.63 Am^{-2}, open circuit voltage of 0.394 V, fill factor of 0.415 and efficiency of 0.228% [32]. Chlorophyll dyes have a low V_{oc} value, which is considered due to the presence of –OH and -O ligands, which cause poor binding so that they do not sufficiently delocalize excited electrons from the dye to the photoanode [32].

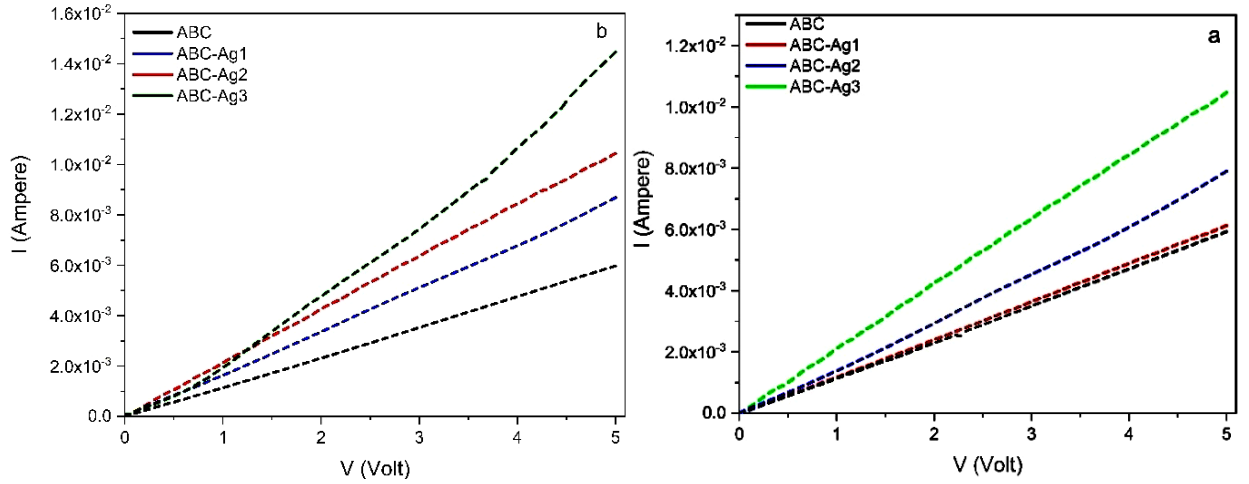

Fig. 5. Curves of current vs. voltage of ABC and ABC/$AgNO_3$ dyes to calculate conductivity under a) dark conditions and b) light irradiation (color online)

Gomesh stated that the thickness of the TiO_2 layer will affect DSSC performance because it tends to increase the amount of dye adsorption. Besides, it also causes the material's resistance to electron transport to be higher, thereby reducing DSSC performance. The photocurrent value is influenced by the acidity of the dye solution [33]. Voc is the difference between the TiO_2 fermi level and the electrolyte redox potential, which depends on the electron recombination rate and the sensitizer adsorption method. Meanwhile, Jsc relies on the amount of dye absorbed on the TiO_2 surface. More dye absorption on the TiO_2 surface produces many photons rapidly converted into electrons, which causes rapid electron injection [34].

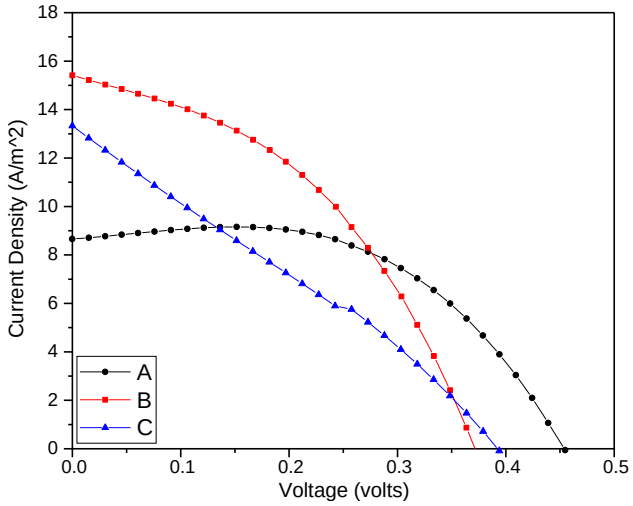

Fig. 6. IV curves of DSSCs using anthocyanin (labeled A), betalain (labeled B), and chlorophyll (labeled C)

These results indicate that anthocyanin and betalain dyes have higher efficiency than chlorophyll because of the interaction between the sensitizer and the TiO_2 film, which has hydrogen bonds influenced by carbonyl and hydroxyl groups. This interaction brings a stronger electron coupling and fast forward and reverse electron transfer reactions, resulting in higher photocurrents [35,11]. Nevertheless, the use of a citric acid solvent to extract dragon fruit skin dye can increase the anthocyanin content and stability of the dye [36].

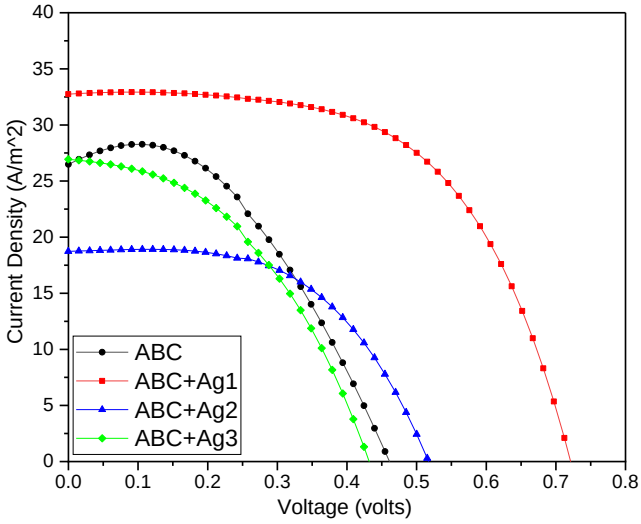

Fig. 7. IV Curve of DSSCs with $AgNO_3$-incorporated ABC dyes (color online)

Table 2 presents that three mixed dyes (ABC) can further increase the DSSC efficiencies than mixtures of two dyes or a single dye, obtaining an efficiency of 0.660%. Mixing three dyes increases efficiency over individual dyes due to the broad absorbance of light energy bands and the presence of complementary single dyes. Besides, a mixture of three dyes can absorb light in three different wavelength regions [37,5].

Mixing three dyes can increase J_{sc}, representing the bonds between dye molecules and TiO_2 particles. Meanwhile, the higher V_{oc} is associated with the suitable conduction band due to the presence of anthocyanin and betalain compounds in the dye [38]. This research also shows that efficiency depends not only on FF but also on other parameters. DSSCs with high FF values do not necessarily have high efficiency. FF is determined by the

level of electron recombination between dye molecules and electrolytes. Low recombination will produce minimum dark current and maximum photoelectron lifetime, resulting in high FF values [39].

Table 1. Conductivity values of ABC and $AgNO_3$-incorporated ABC dyes

Dye Materials	σ (dark) $(\Omega^{-1}m^{-1})$	σ (bright) $(\Omega^{-1}m^{-1})$	Δσ $(\Omega^{-1}m^{-1})$
ABC	0.4678	0.9149	0.4471
ABC-Ag1	0.5423	1.5498	1.0075
ABC-Ag2	0.6776	1.8935	1.2159
ABC-Ag3	0.7947	2.1052	1.3105

Table 2. Electrical properties of DSSCs with single dye, mixed dye, and $AgNO_3$-incorporated mixed dye

Dye	V_{OC} (V)	J_{sc} (Am^{-2})	*FF*	η (%)
A (H polyrhizus)	0.469	9.04	0.456	0.193
B (B Glabra)	0.379	15.86	0.375	0.225
C (Mutilisima)	0.394	13.63	0.415	0.228
A B C	0.460	26.80	0.535	0.660
ABC-Ag1	0.727	32.65	0.689	1.635
ABC-Ag2	0.535	19.64	0.556	0.584
ABC-Ag3	0.433	25.95	0.444	0.498

Table 2 and Fig. 7 reveal that $AgNO_3$-incorporated ABC with 3 mM Ag concentration produced the best DSSC efficiency among other dye modifications. However, the efficiency value decreases along with the higher concentration of $AgNO_3$. This is because Ag has good conductivity properties, so the higher concentration added may increase the conductivity of the TiO_2 photoanode layer in DSSC. Even though it is hybridized into the dye, adding $AgNO_3$ with a higher concentration may cause aggregation in dyes [11]. The increase in the concentration causes the surface of the active area to be blocked by large amounts of Ag so that it becomes a recombination center. Consequently, it decreases J_{sc} and V_{oc}, thereby reducing the efficiency of DSSC [14].

Onimisi also reported that $AgNO_3$ can be ionized by the electrolyte and oxidized to become Ag^+ ions, causing increased electron-holes recombination and reduced charge carriers number, resulting in decreased J_{sc} and V_{oc}. In addition, higher concentrations can agglomerate to form larger Ag ion clusters with lower electron storage capability, thereby reducing V_{oc} [40, 41]. This is also supported by Usha's research results that the addition of Ag with an excessive concentration can enhance the conductivity of the TiO_2 semiconductor so that it will prevent the electrolyte from making direct contact with the conductive substrate, resulting in a lower J_{sc} value [30]. Therefore, ABC dye with the lowest concentration of $AgNO_3$ doping ($3x10^{-3}$ M) is a good combination for optimum efficiency.

Concerning the bandgap, the addition of $AgNO_3$ affects the conductivity value of the semiconductor layer used. As a result, the resulting bandgap will be smaller, affecting the value of the DSSC efficiency [29]. As in this study, the addition of Ag ions significantly increased the conductivity of the dye solution, reduced the energy band gap value, and declined the light absorption ability of the dye. This causes the process of excitation and electron transport in the cell to be ineffective and not optimal, thereby reducing the performance and efficiency of DSSC. The addition of Ag ion concentration in ABC dye causes a decrease in efficiency called the metal bulk effect, where the DSSC performance reaches optimal efficiency at a certain amount of concentration and decreases at a higher concentration level [9]. The addition of $AgNO_3$ with a large concentration produces a relatively narrow energy bandgap value, causing electrons to move fastly from HOMO to LUMO, which can overlap, thereby reducing the efficiency.

4. Conclusions

DSSC devices have been successfully fabricated using natural anthocyanin, betalain, and chlorophyll dyes and their mixture. $AgNO_3$ was incorporated into three mixed dyes (ABC) with various concentrations to improve the DSSC performance. The results revealed that ABC dye exhibited the best DSSC performance among the dye mixtures, with an efficiency of up to 0.660%. Further, the Ag doping could enhance its performance. It demonstrated that $AgNO_3$-incorporated ABC, with the lowest Ag concentration, was the best dye modification to produce with an efficiency of 1.635 %. Indeed, the higher Ag concentration doping resulted in declined DSSC efficiencies. The addition of excessive Ag causes a decrease in current and voltage due to the metal bulk effect, thereby reducing the efficiency.

Acknowledgments

This activity is supported by the Research and Community Service Institute of Sebelas Maret University through the HRG Grant Program Contracts Number: 194.2/UN27.22/PT.01.03/2024

Declaration of interest

The authors declare that there is no conflict of interest to disclose.

References

[1] M. Bhogaita, A.D. Shukla, R. P. Nalini, J. Sol. Energy **137**(6), 212 (2016).
[2] M. A. Al-alwani, A. B. Mohamad, N. A. Ludin, A. A. H. Kadhum, K. Sopian, Renew. Sustain.

Energy Rev. **65**, 183 (2016).
[3] A. Ashok, S. E. Mathew, S. B. Shivaram, S. A. Shankarappa, S. V. Nair, M. Shanmugam, J. Sci. Adv. Mater. Devices **3**(2), 213 (2018).
[4] F. Kabir, S. N. Sakib, N. Matin, Optik **181**, 458 (2019).
[5] D. Sinha, D. De, A. Ayaz, Sādhanā **45**(1), 1 (2020).
[6] D. Eli, G. P. Musa, D. Ezra, Journal of Energy and Natural Resources Law **5**(5), 53 (2016).
[7] G. Richhariya, A. Kumar, P. Tekasakul, B. Gupta, Renewable and Sustainable Energy Review **69**, 705 (2017).
[8] D. D. Pratiwi, F. Nurosyid, A. Supriyanto, R. Suryana, J. Phys. Conf. Ser. **776**(1), 012007 (2016).
[9] D. D. Pratiwi, F. Nurosyid, K. Kusumandari, A. Supriyanto, R. Suryana, AIP Conf. Proc. **2014**, 020066 (2014).
[10] F. Khojasteh, M. R. Mersagh, H. Hashemipour, J. Alloys Compd. **890**(1), 161709 (2022).
[11] A. Supriyanto, D. Galih, M. Khairul, B. Ahmad, A. Handono, F. Ramadhani, Optik **231**(1), 1 (2021).
[12] A. K. Gupta, P. Srivastava, L. Bahadur, Appl. Phys. A **122**(8), 1 (2016).
[13] D. Samson, T. Adeeko, E. Makama, Int. J. Curr. Res. Acad. Rev. **5**(12), 15 (2017).
[14] P. Faqih, F. Nurosyid, T. Kusumaningsih, AIP Conf Proc. **2237**(7), 1 (2020).
[15] E. K. Palupi, R. Umam, B. A. Bibin, S. Hidetoshi, Y. Brian, A. Husin, Ferroelectrics **540**(1), 1 (2019).
[16] B. Y. Muryani, F. Nurosyid, Kusumandari, AIP Conf Proc. **2237**(1), 1 (2020).
[17] F. I. Pote, A. Supriyanto, F. Nurosyid, D. Kurniawan, J. Phys. Theor. Appl. **3**(2), 69 (2019).
[18] K. U. Isah, A. Y. Sadik, B. J. Jolayemi, Eur. J. Appl. Sci. **9**(3), 140 (2017).
[19] A. R. Hernandez-Martinez, M. Estevez, S. Vargas, F. Quintanilla, R. Rodriguez, Int. J. Mol. Sci. **12**(9), 5565 (2011).
[20] Q. S. Wei, M. F. Aizat, A. Diyanti, W. M. F. Ishak, H. Salleh, K. N. S. W. S. Wong, H. K. Adli, AIP Conf. Proc. **2068**(1), 1 (2019).
[21] O. Adedokun, K. Titilope, A. O. Awodugba, Int. J. Eng. Technol. **2**(2), 34 (2016).
[22] R. Ramamoorthy, N. Radha, G. Maheswari, S. Anandan, S. Manoharan, R. Victor Williams, J. Appl. Electrochem. **46**(9), 929 (2016).
[23] N. Y. Amogne, D. W. Ayele, Y. A. Tsigie, Renewable Sustainable Energy Rev. **9**(4), 1 (2020).
[24] W. A. Dhafina, M. Z. Daud, H. Salleh, Optik **207**(4), 163808 (2020).
[25] N. Patni, S. G. Pillai, P. Sharma, Int. J. Energy Res. **44**(13), 10846 (2020).
[26] P. K. Singh, V. K. Shukla, Mater. Today Proc. **49**(8), 3235 (2022).
[27] Y. E. Du, Q. Feng, C. Chen, Y. Tanaka, X. Yang, ACS Appl. Mater. Interfaces **6**(18), 16007 (2014).
[28] A. Kubiak, K. Siwińska-Ciesielczyk, Z. Bielan, A. Zielińska-Jurek, T. Jesionowski, Adsorption **25**(2), 309 (2019).
[29] D. G. Saputri, A. Supriyanto, M. K. B. Ahmad, F. Ramadhani, J. Phys. Conf. Ser. **2190** (1), 012036 (2022).
[30] K. Usha, P. Kumbhakar, B. Mondal, Mater. Sci. Semicond. Process. **43**, 17 (2016).
[31] U. A. Kamarulzaman, M. Y. A. Rahman, M. S. S. U'ait, A. A. Umar, Optik **276**(4), 170658 (2023).
[32] D. Sengupta, B. Mondal, K. Mukherjee, Spectrochim. Acta A Mol. Biomol. Spectrosc. **148**, 85 (2015).
[33] N. Gomesh, R. Syafinar, M. Irwanto, Y. M. Irwan, M. Fareq, U. Hashim, N. Mariun, Appl. Mech. Mater. **793**(2), 450 (2015).
[34] G. Calogero, G. Di Marco, Sol. Energy Mater Sol. Cells **92**(11), 1341 (2008).
[35] A. Torchani, S. Saadaoui, R. Gharbi, M. Fathallah, Curr. Appl. Phys. **15**(3), 307 (2015).
[36] N. Prabavathy, S. Shalini, R. Balasundaraprabhu, D. Velauthapillai, S. Prasanna, G. Balaji, N. Muthukumarasamy, Int. J. Energy Res. **42**(2), 790 (2018).
[37] A. Ayaz, D. Sinha, D. De, Int. J. Innov. Technol. Explor. Eng. **9**(7), 453 (2020).
[38] M. Peymannia, K. Gharanjig, A. M. Arabi, Int. J. Energy Res. **44**(18), 309 (2019).
[39] K. Inbarajan, S. Sowmya, B. Janarthanan, Opt. Mater. **129**, 112487 (2022).
[40] M. Y. Onimisi, D. Eli, S. G. Abdu, H. O. Aboh, E. Jonathan, Am. Chem. Sci. J. **13**(3), 1 (2016).
[41] Takai, P. V. Kamat, ACS Nano **5**(9), 7369 (2011).

*Corresponding author: fahrunurosyid@staff.uns.ac.id